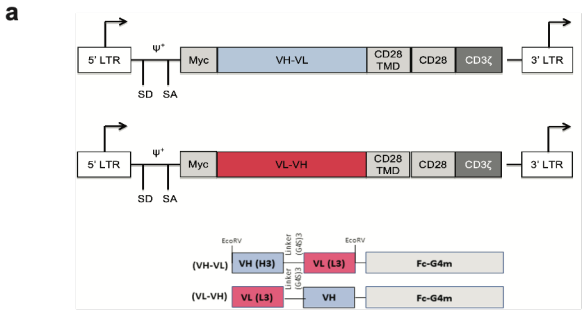

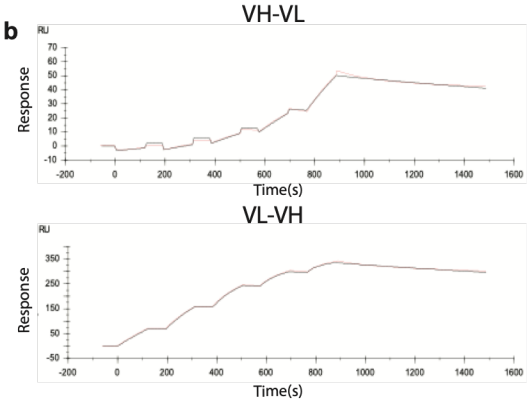

c

	KD (M)	Ka (1/Ms)	kd (1/s)	ED50 (ng/ml)
IgG	1.31E-09	2.14E+05	2.81E-04	37
VH-VL	9.79E-07	1.87E+03	1.83E-03	3952
VL-VH	3.26E-09	7.77E+04	2.53E-04	34

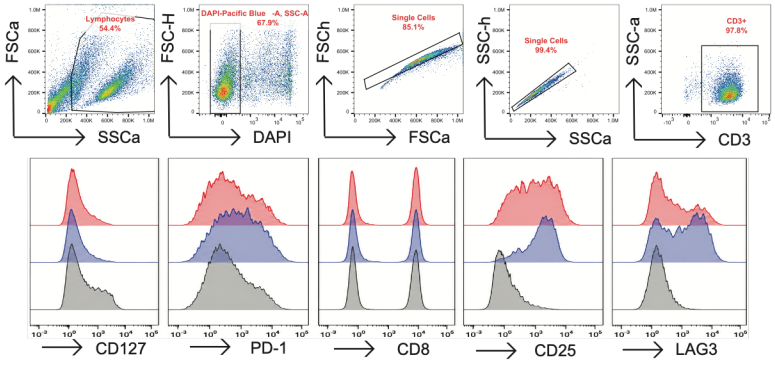

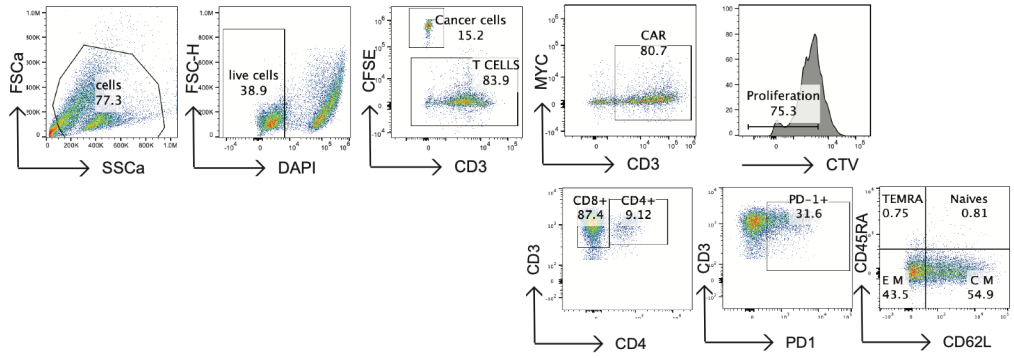

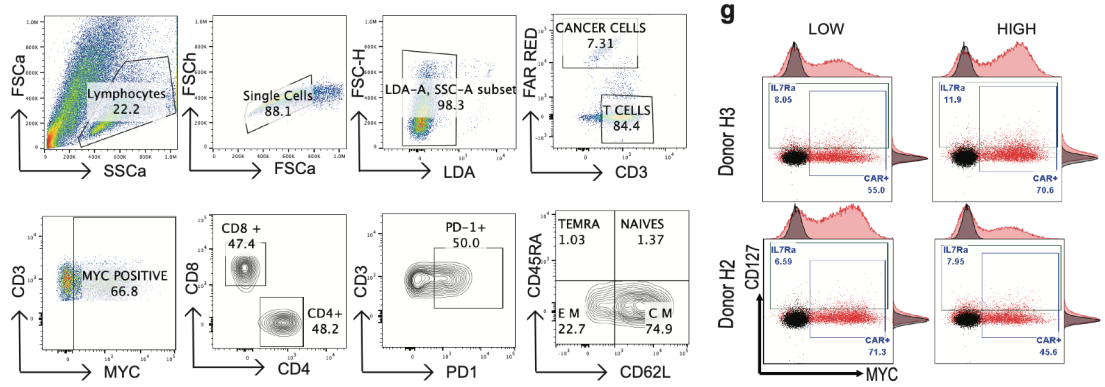

Supplementary Fig. S1. Anti-CD127 scFv target binding characteristics and representative flow cytometry gating strategy. a, Schematic illustrating variable heavy (VH) and variable light (VL) chain positioning in the respective scFvs used in the anti-CD127 CAR constructs shown in Fig. 1a and the original monoclonal antibody formats of the scFvs (bottom). **b,** Line plots displaying the kinetics of anti-CD127 monoclonal antibody binding to its target in 2 scFv formats: VH-VL (top panel) and VL-VH (bottom panel). Binding kinetics were determined in 1 experiment. **c,** Tabulated data illustrating differences in the measurements of the equilibrium dissociation constant (KD), rate of association constant (Ka), rate of equilibrium dissociation constant (Kd), and median effective dose (ED50) concentration of the 2 scFv formats, compared with control IgG. Data in b,c were obtained in 1 experiment. **d,** Representative flow plots illustrating the gating strategy used to locate T cells on day 4 after transduction and corresponding histogram plots of different cell surface markers of data shown in Supplementary Fig. S2b,c. Data are representative of 3 independent donors. **e,** Gating strategy used to identify CTV^+ $CD3^+$ and/or MYC^+ cells collected at serial time points from the accumulation assay shown in Supplementary Fig. S2d,e. **f,** Gating strategy used to identify MYC^+ $CD3^+$ FAR/RED^- CAR T cells collected at serial time points from the repeated antigen-stimulation assays shown in Supplementary Fig. S2f,g. CM, central memory; EM, effector memory; FSC-A, forward scatter area; FSC-H, forward scatter height; LTR, long terminal repeat; SA, splice acceptor; SD, splice donor; SSC-A, side scatter area; SSC-H, side scatter height; TMD, transmembrane domain. **g,** Flow-cytometry plots showing MYC^+ CAR T-cell percentages in low-affinity and high-affinity products from 2 donors. Source data are provided as source data file.

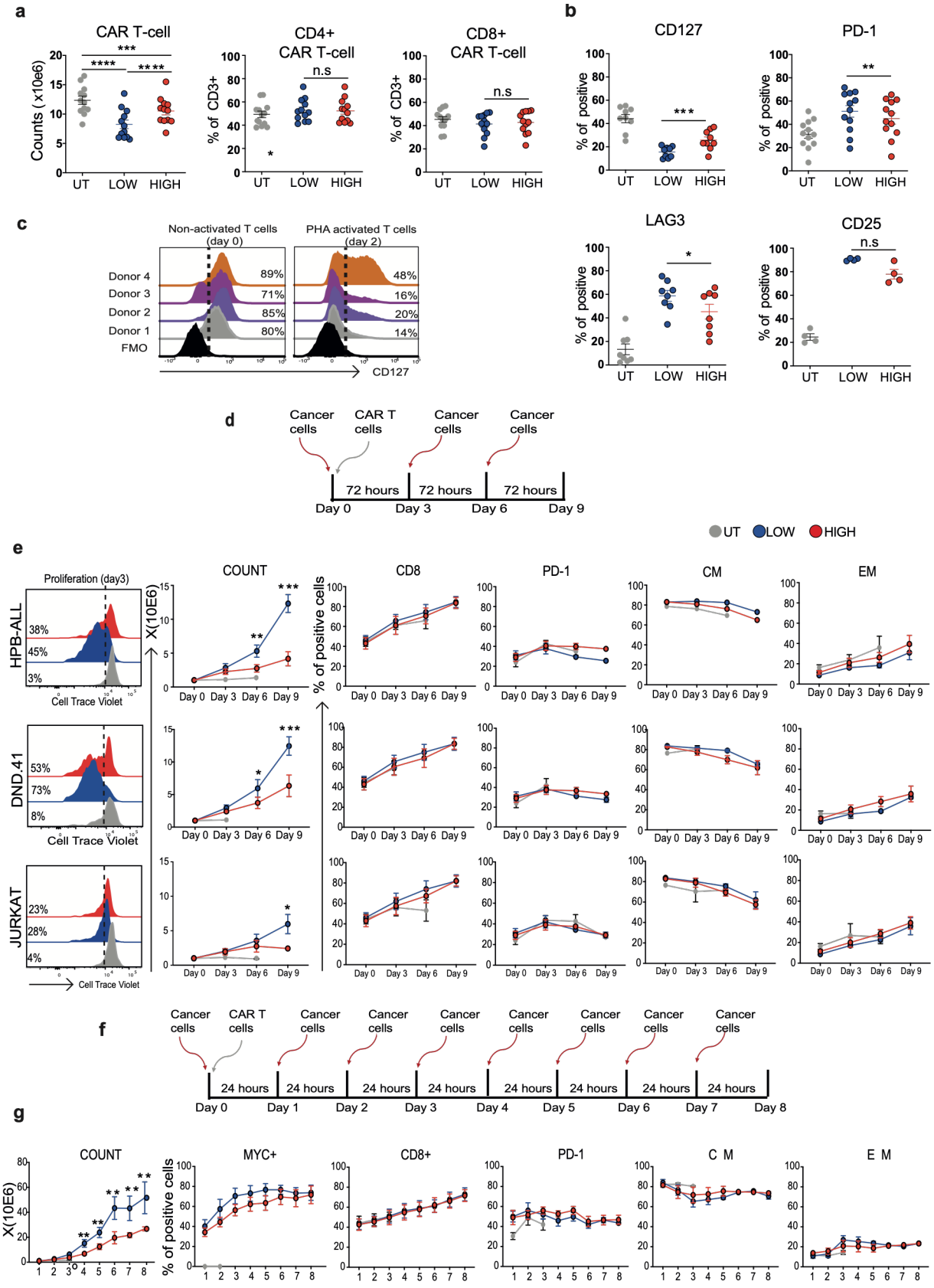
a
CAR T-cell
Counts (x10e6)
UT
LOW
HIGH
CD4+ CAR T-cell
% of CD3+
n.s
CD8+ CAR T-cell
b
CD127
% of positive
PD-1
c
Non-activated T cells (day 0)
PHA activated T cells (day 2)
Donor 4
Donor 3
Donor 2
Donor 1
FMO
89%
71%
85%
80%
48%
16%
20%
14%
CD127
LAG3
CD25
d
Cancer cells
CAR T cells
72 hours
Day 0
Day 3
Day 6
Day 9
e
UT
LOW
HIGH
Proliferation (day3)
HPB-ALL
DND.41
JURKAT
Cell Trace Violet
COUNT
X(10E6)
CD8
% of positive cells
CM
EM
f
24 hours
Day 0
Day 1
Day 2
Day 3
Day 4
Day 5
Day 6
Day 7
Day 8
g
COUNT
MYC+
CD8+
C M
E M

Supplementary Fig. S2. Anti-CD127 LOW CAR T cells are more fratricidal and proliferative *in vitro*, compared with UT or HIGH CAR T cells. a, Dot plots showing cell counts of UT, LOW CAR, and HIGH CAR T cells and phenotyping analysis showing the percentage of $CD3^+$ cells expressing CD4 and CD8 at day 4 after transduction. Data are from 12 independent donors per group and are presented as mean ± standard deviation. Statistical analysis was performed using multiple unpaired two-tailed Student's *t*-tests. p values: CAR T-cell counts, UT vs LOW, $p = 0.0005$; LOW vs HIGH, $p = 0.0295$. **b,** Dot plots showing the frequency of UT and LOW or HIGH CAR T cells with expression of CD127, PD-1, LAG3, and CD25 at day 4 after transduction. Number of donors: CD127 (n = 9 donors), PD-1 (n = 12 donors), LAG3 (n = 8 donors), and CD25 (n = 4 donors). Data are presented as mean ± standard deviation. Statistical analysis was performed using multiple unpaired two-tailed Student's *t*-tests. p values: CD127, UT vs LOW, $p = 0.0000015$; LOW vs HIGH, $p = 0.0053$; PD-1, UT vs LOW, $p = 0.0039$. **c,** Histogram plots illustrating the expression of CD127 in 4 healthy donor–derived T cells on day 0 (nonactivated) and day 2 after phytohemagglutinin (PHA) activation. Data are representative of 3 independent donors. **d,** Schematic of the repeated antigen-stimulation assay involving coculture of target cells (HPB-ALL, DND.41, or Jurkat) with CTV-labeled anti-CD127 CAR T cells on day 0 at an E:T ratio of 1:1 and with the addition of fresh target cells every 72 h for 2 rounds. **e,** Representative histogram plots showing reduced CTV signal, indicating cell proliferation, on day 3 of coculture of LOW and HIGH CAR T cells with HPB-ALL (top panel), DND.41 (middle panel), and Jurkat (bottom panel) target cells. Histogram plots are shown with summary line plots illustrating cell counts and the proportion of cells expressing CD8 and PD-1 and displaying a central memory (CM) or effector memory (EM) cell phenotype among MYC^+ cells after sequential rechallenge with the respective tumor cell types indicated. Data are representative of 2 independent donors and are presented as mean ± standard deviation. **f,** Schematic of the repeated antigen-stimulation assay with continuous antigen exposure to DND.41 target cells every 24 h at an E:T ratio of 1:1 for 8 rounds. **g,** Corresponding line plots showing cell counts and the proportion of cells expressing CAR (percentage of MYC^+), along with the percentages of cells with expression of CD8 or PD-1 and a central memory or effector memory cell phenotype among MYC^+ cells over the course of the experiment. Data are from 3 independent donors and are presented as mean ± standard deviation. Statistical analysis was performed using multiple unpaired two-tailed Student's *t*-tests. Exact p value: Round 5, $p = 0.0094$. FMO, fluorescence minus one; ns, not significant. Source data are provided as source data file.

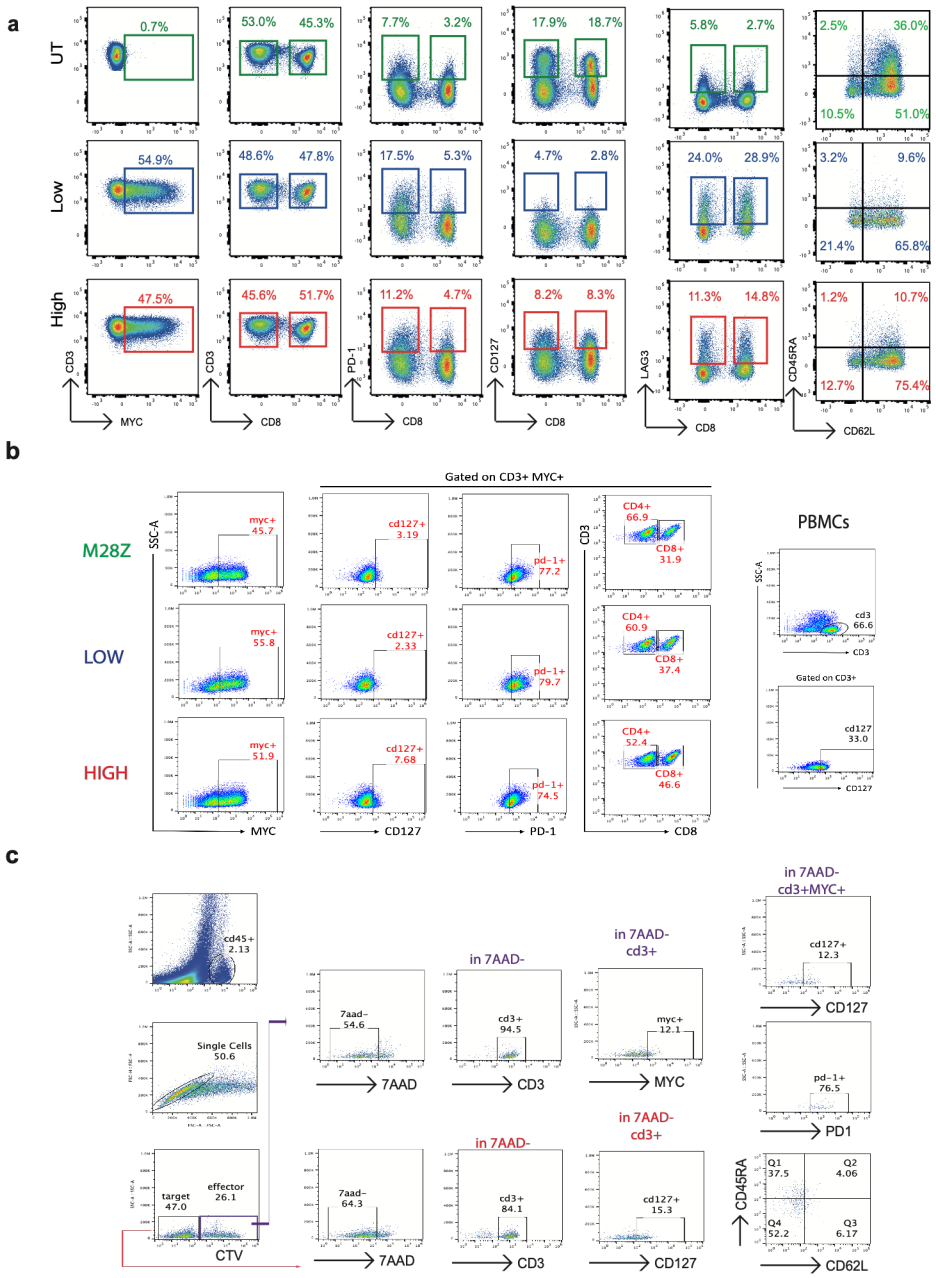

Supplementary Fig. S3. Gating strategy and cell phenotype plots of the data presented in Fig. 2 and Supplementary Fig. S4. a, Representative flow cytometry plots showing phenotype assessment of pre-administration LOW and HIGH CAR T cells used in the *in vivo* study, showing equivalent CAR transduction efficiency and similar differentiation of $CD4^+$ and $CD8^+$ T cells and distribution of memory cell phenotypes. **b,c,** Gating strategy for the flow cytometry data presented in Supplementary Fig. S4e,f. FSC-H, forward scatter height; SSC-A, side scatter area.

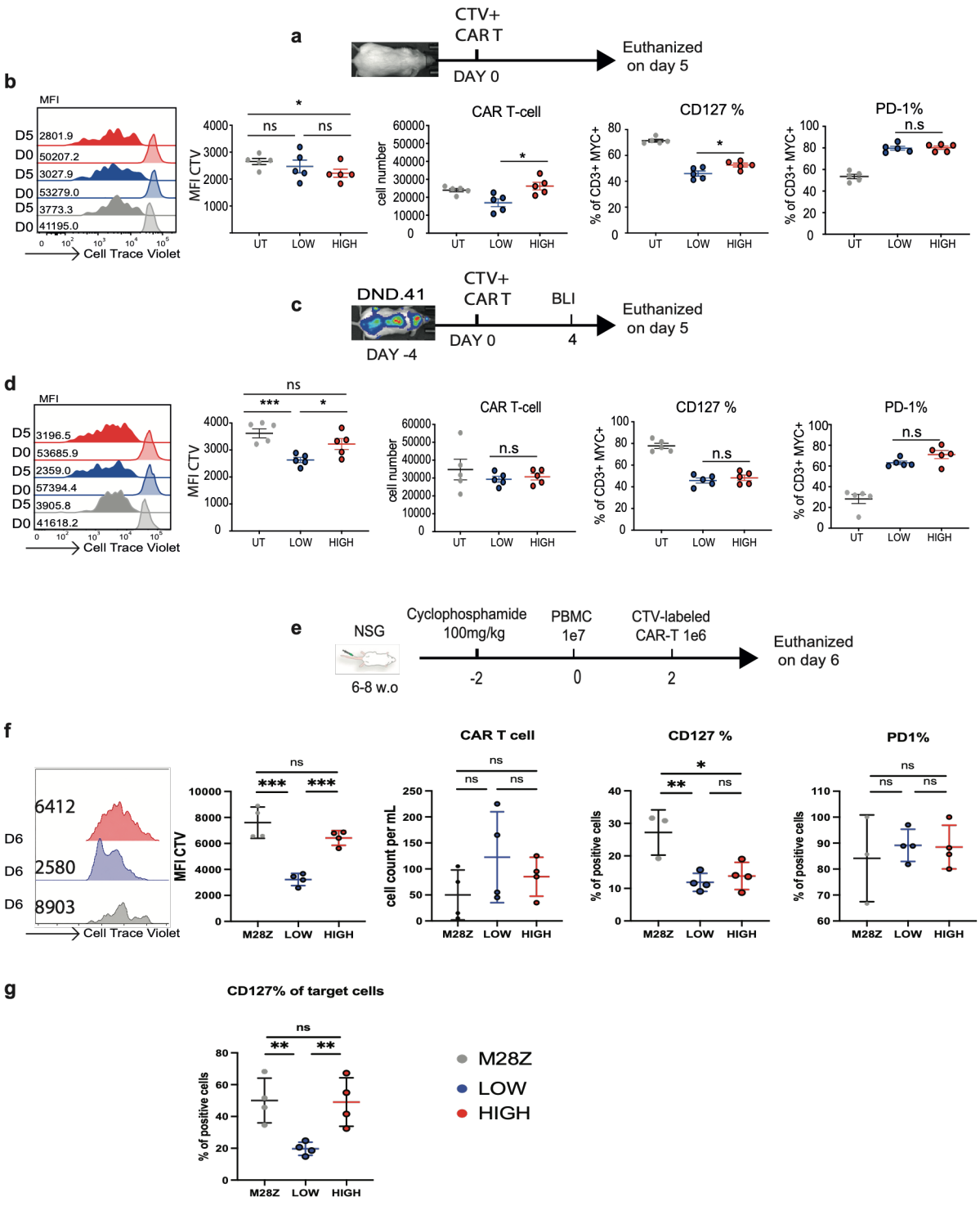
a
CTV+
CAR T
DAY 0
Euthanized
on day 5
b
MFI
D5 2801.9
D0 50207.2
D5 3027.9
D0 53279.0
D5 3773.3
D0 41195.0
Cell Trace Violet
MFI CTV
ns
ns
*
UT
LOW
HIGH
CAR T-cell
cell number
*
CD127 %
% of CD3+ MYC+
*
PD-1%
n.s
c
DND.41
CTV+
CAR T
BLI
DAY -4
DAY 0
4
Euthanized
on day 5
d
MFI
D5 3196.5
D0 53685.9
D5 2359.0
D0 57394.4
D5 3905.8
D0 41618.2
Cell Trace Violet
ns
***
*
CAR T-cell
n.s
CD127 %
n.s
PD-1%
n.s
e
NSG
6-8 w.o
Cyclophosphamide
100mg/kg
PBMC
1e7
CTV-labeled
CAR-T 1e6
-2
0
2
Euthanized
on day 6
f
6412
D6
2580
D6
8903
Cell Trace Violet
MFI CTV
ns
***
***
M28Z
LOW
HIGH
CAR T cell
cell count per mL
CD127 %
% of positive cells
*
**
ns
PD1%
g
CD127% of target cells
% of positive cells
**
**
M28Z
LOW
HIGH

Supplementary Fig. S4. Assessment of the effects of fratricide among LOW and HIGH CAR T cells *in vivo*. a, Schematic of the *in vivo* study design. Mice were intravenously administered $3x10^6$ CTV-labeled CAR T cells. On day 5, mice were euthanized, and CAR T-cell phenotype from peripheral blood was assessed by flow cytometric analysis. **b,** Representative histogram plots and quantification of CTV-BV421 signal (MFI of CTV) showing *in vivo* proliferation of UT, LOW CAR, and HIGH CAR T cells by day 5, depicted by a reduced CTV signal, compared with day 0. Relative levels of accumulation (cell number) and the percentage of cells expressing CD127 and PD-1 are also shown. n = 5 mice per cohort. **c,** Schematic of the *in vivo* study design. Mice were inoculated with $3x10^6$ DND.41-effLuc cells on day -4, followed by intravenous administration of $3x10^6$ (CTV-labeled) CAR T cells. On day 5 after administration of CAR T cells, and CAR T-cell phenotype from bone marrow was assessed by flow cytometric analysis. **d,** Assessment of the proliferation (MFI of CTV) and accumulation (cell number) of cells and the percentage of cells with expression of CD127 and PD-1 in bone marrow harvested from cancer cell–bearing mice. n = 5 mice per cohort**. e,** Schematic of the *in vivo* study design. Mice were treated with 100 mg/kg cyclophosphamide intraperitoneally on day -2 and were intravenously administered $1x10^7$ healthy donor–derived PBMCs on day 0. Two days later, on day 2, mice were intravenously administered $1x10^6$ autologous CAR T cells (PBMC donor derived) labeled with CTV. On day 6, all mice were euthanized, and CAR T-cell phenotype from bone marrow was analyzed by flow cytometric analysis. **f,** Assessment of the proliferation (MFI of CTV), accumulation (cell number), and percentage of cells with expression of CD127 and PD-1 in bone marrow harvested from autologous PBMC–bearing mice**.** Data are representative of a pool of 4 mice per group and are presented as mean ± standard error of the mean. Statistical analysis was performed using an unpaired two-tailed Student's *t*-test. p values: CTV MFI, M28Z vs LOW, $p = 0.0005$; LOW vs HIGH, $p = 0.00013$. CD127, M28Z vs LOW, $p = 0.0239$; M28Z vs HIGH, $p = 0.0093$. **g,** Percentage of PBMC target cells (CTV-) expressing CD127 (percentage CD127) harvested from bone marrow on day 6. Data are representative of a pool of 4 mice per group. Data are shown as mean ± standard error of the mean. *P* values: M28Z vs LOW, $p = 0.0060$; LOW vs HIGH, $p = 0.0099$. D, day; ns, not significant. Source data are provided as source data file.

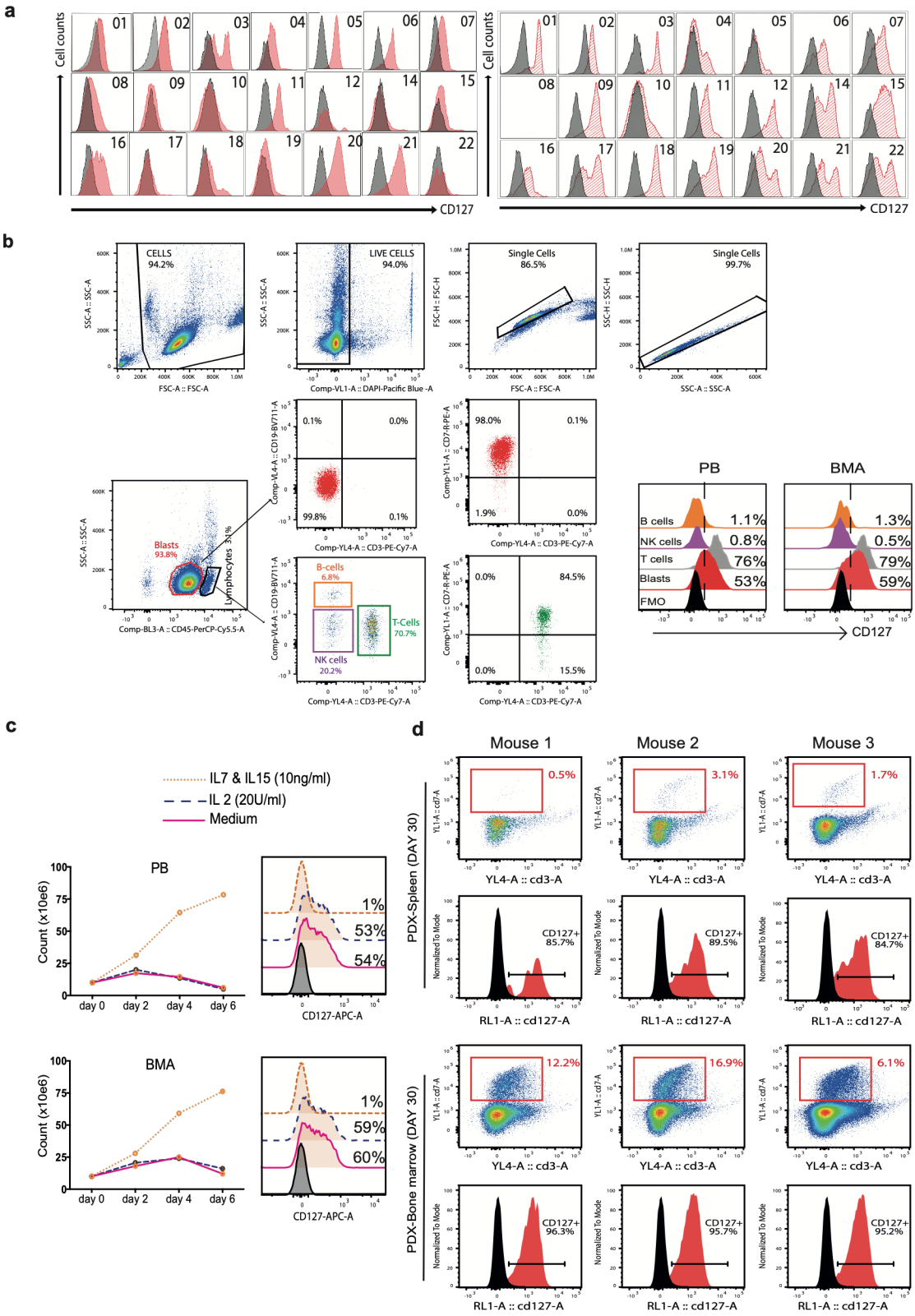
a
Cell counts
CD127
b
CELLS
94.2%
LIVE CELLS
94.0%
Single Cells
86.5%
Single Cells
99.7%
Blasts
93.8%
Lymphocytes 3.1%
B-cells
6.8%
T-Cells
70.7%
NK cells
20.2%
PB
BMA
B cells
NK cells
T cells
Blasts
FMO
1.1%
0.8%
76%
53%
1.3%
0.5%
79%
59%
c
IL7 & IL15 (10ng/ml)
IL 2 (20U/ml)
Medium
PB
BMA
Count (x10e6)
day 0
day 2
day 4
day 6
CD127-APC-A
1%
53%
54%
1%
59%
60%
d
Mouse 1
Mouse 2
Mouse 3
PDX-Spleen (DAY 30)
PDX-Bone marrow (DAY 30)
0.5%
3.1%
1.7%
12.2%
16.9%
6.1%
CD127+
85.7%
CD127+
89.5%
CD127+
84.7%
CD127+
96.3%
CD127+
95.7%
CD127+
95.2%
YL4-A :: cd3-A
RL1-A :: cd127-A

Supplementary Fig. S5. Primary blast and normal T cells isolated from patients with T-ALL show expression of CD127, and primary blast cells can be expanded in NSG mice *in vivo*. a, Histogram plots showing expression of CD127 on primary blasts (red histograms) and normal T cells (red dashed histograms) isolated from 21 independent patient samples with T-ALL (pediatric and adult), as listed in Supplementary Table 1. **b,** Flow cytometry plots showing the gating strategy to differentiate normal T cells ($CD45^{hi}$ $CD3^{+}$ $CD7^{+}$) from malignant T cells ($CD45^{dim}$ $CD3^{-}$ $CD7^{+}$) isolated from the samples from patient 2. Histogram overlay plots showing the percentage of cells expressing CD127 on the cell surface of normal B-cell, natural killer cell, and T-cell blasts and malignant T-cell blasts harvested from patient 2, along with peripheral blood (PB) and bone marrow aspirate (BMA). **c,** Line plots showing absolute cell number (count) and histogram plots showing expression of CD127 on the cell surface of blasts cultured *ex vivo* in medium alone or in medium supplemented with IL7 or IL15 (10 ng/mL) or IL2 (20 U/mL). Data are representative of 3 independent patient samples. **d,** Representative flow cytometry plots showing the identification of blast cells in spleen (top panels) and bone marrow (bottom panels) from NSG mice on day 30 after intravenous administration of $1x10^6$ blasts via tail vein injection. Histogram plots showing the percentage of cells expressing CD127 on the cell surface of *in vivo*–expanded blasts displayed above, respectively. Data are representative of 3 donors. APC Allophycocyanin; FMO, fluorescence minus one; FSC-A, forward scatter area; FSC-H, forward scatter height; NK, natural killer; PDX, patient-derived xenograft; SSC-A, side scatter area.

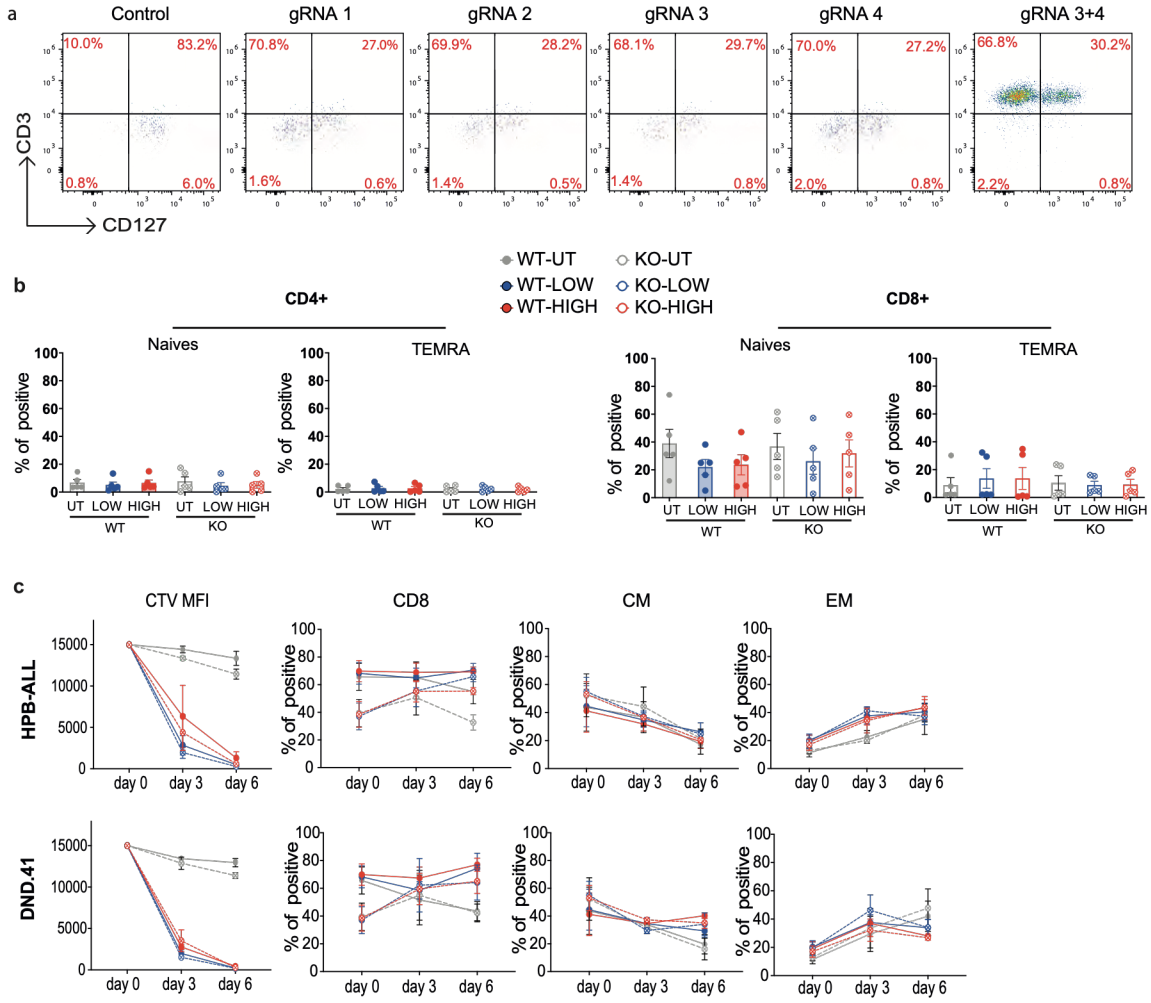

Supplementary Fig. S6. Supplementary data supporting the data presented in Fig. 4. a, Representative flow cytometry density plots showing the percentage of cells expressing CD127 after *CD127* gene knockout by use of CRISPR-Cas9 using 4 different guide RNAs (gRNAs), compared with control cells. Data are representative of 5 independent donors. **b,** Bar graphs showing differentiated states of CAR T cells, as indicated by the distribution of either CD4- or CD8-naive ($CD45RA^+$ $CD62L^+$) or TEMRA ($CD45RA^+$ $CD62L^-$) phenotypes on day 4 after transduction with or without *CD127* gene knockout. Data are representative of 5 independent donors. **c,** Corresponding data plots showing the functional persistence and accumulation of anti-CD127 CAR T cells, as indicated by the proliferation (MFI of CTV) of CAR T cells and the percentage of CD8 T cells, respectively, and the distribution of central memory (CM) and effector memory (EM) cell phenotypes after coculture of CTV-labeled CAR T cells with T-ALL cancer cell lines for up to 6 days. Data are representative of 3 independent donors. KO, knockout; WT, wild-type. Source data are provided as source data file.

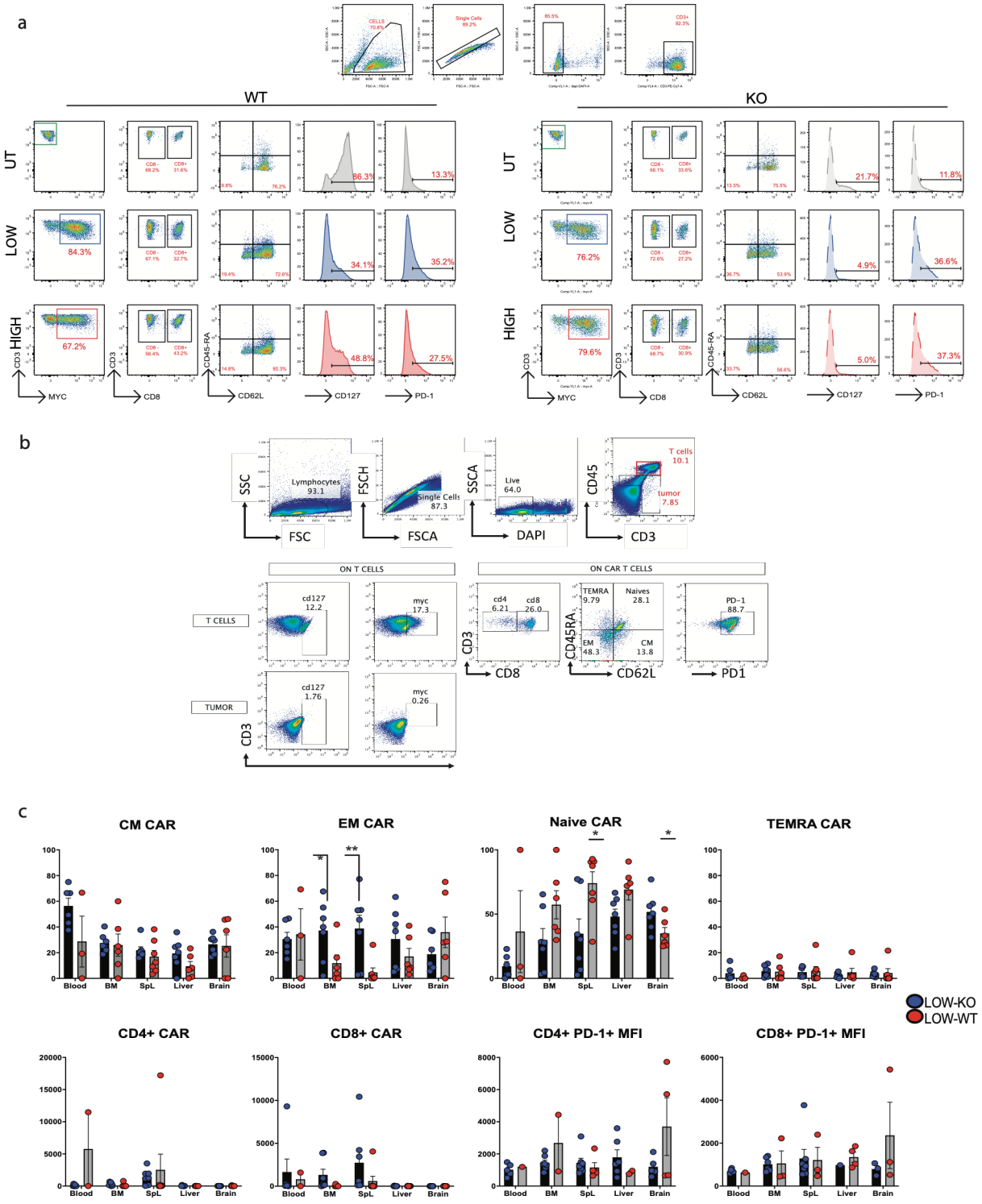
a
WT
KO
UT
LOW
HIGH
84.3%
67.2%
76.2%
79.6%
86.3%
13.3%
34.1%
35.2%
48.8%
27.5%
21.7%
11.8%
4.9%
36.6%
5.0%
37.3%
MYC
CD8
CD62L
CD127
PD-1
b
Lymphocytes 93.1
Single Cells 87.3
Live 64.0
T cells 10.1
tumor 7.85
FSC
FSCA
DAPI
CD3
ON T CELLS
ON CAR T CELLS
T CELLS
TUMOR
cd127 12.2
myc 17.3
cd4 6.21
cd8 26.0
TEMRA 9.79
Naives 28.1
EM 48.3
CM 13.8
PD-1 88.7
cd127 1.76
myc 0.26
CD45RA
PD1
c
CM CAR
EM CAR
Naive CAR
TEMRA CAR
CD4+ CAR
CD8+ CAR
CD4+ PD-1+ MFI
CD8+ PD-1+ MFI
Blood
BM
SpL
Liver
Brain
LOW-KO
LOW-WT

Supplementary Fig. S7. Supplementary data supporting the data presented in Fig. 5 and Supplementary Fig. S8. a, Flow cytometry dot plots showing phenotype assessment of pre-administration CAR T cells used in the *in vivo* study. CAR transduction efficiency is shown as the percentage of MYC, distribution of T-cell subsets by $CD8^+$ and $CD8^-$ ($CD4^+$) staining, and cell differentiation phenotypes by CD45RA and CD62L staining. Histogram plots show CRISPR-Cas9 knockout efficiency by the percentage of CD127, and expression of PD-1 of wild-type and knockout LOW and HIGH CAR T cells are compared with those of UT T-cell controls. Data are representative of 3 independent donors. **b,** Gating strategy of the flow cytometric analysis performed in Fig. 5g and representative flow cytometry dot plots showing the percentage of total T cells ($CD45^+$ $CD3^+$) harvested from various organs, including spleen, bone marrow, blood, brain, liver, and intestine. Data are representative of 3 independent donors. **c,** Summary plot of flow cytometry data showing assessment of differentiation status of CAR T cells in blood, bone marrow (BM), spleen (SPL), liver, and brain harvested from day 53 to 126 after administration of CAR T cells. Data are representative of a pool of 6 to 7 mice per group and were analyzed using multiple 2-tailed unpaired Student's *t* tests. Data are shown as mean ± standard deviation. Number of mice: blood, LOW-KO (n = 6), LOW-WT (n = 3); BM, LOW-KO (n = 7), LOW-WT (n = 6); spleen, LOW-KO (n = 7), LOW-WT (n = 7); liver, LOW-KO (n = 7), LOW-WT (n = 6); brain, LOW-KO (n = 7), LOW-WT (n = 6). p values: EM CAR, BM, $p = 0.0448$; EM CAR, SpL, $p = 0.0090$; Naïve CAR, SpL, $p = 0.0203$; Naïve CAR, Brain, $p = 0.0432$. CM, central memory; EM, effector memory; FSC, forward scatter; FSC-A, forward scatter area; FSC-H, forward scatter height; KO, knockout; ns, not significant; SSC, side scatter; SSC-A, side scatter area; WT, wild-type. Source data are provided as source data file.

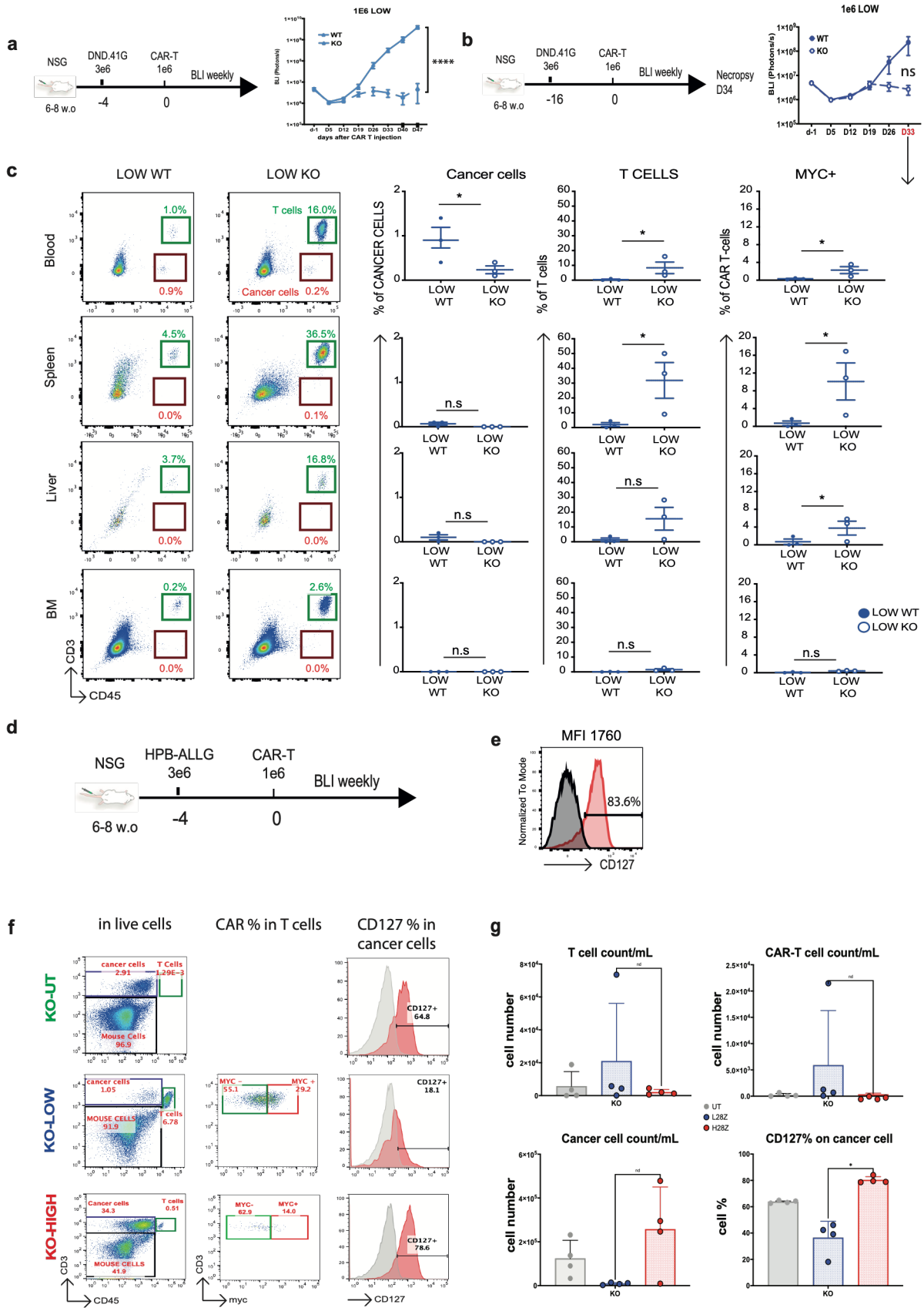
a
NSG
6-8 w.o
DND.41G 3e6
-4
CAR-T 1e6
0
BLI weekly
1E6 LOW
WT
KO
****
days after CAR T injection
b
NSG
6-8 w.o
DND.41G 3e6
-16
CAR-T 1e6
0
BLI weekly
Necropsy D34
1e6 LOW
WT
KO
ns
c
LOW WT
LOW KO
Cancer cells
T CELLS
MYC+
Blood
Spleen
Liver
BM
1.0%
0.9%
T cells 16.0%
Cancer cells 0.2%
4.5%
0.0%
36.5%
0.1%
3.7%
0.0%
16.8%
0.0%
0.2%
0.0%
2.6%
0.0%
CD3
CD45
% of CANCER CELLS
% of T cells
% of CAR T-cells
LOW WT
LOW KO
n.s
*
d
NSG
6-8 w.o
HPB-ALLG 3e6
-4
CAR-T 1e6
0
BLI weekly
e
MFI 1760
Normalized To Mode
83.6%
CD127
f
in live cells
CAR % in T cells
CD127 % in cancer cells
KO-UT
KO-LOW
KO-HIGH
cancer cells 2.91
T Cells 1.29E-3
Mouse Cells 96.9
CD127+ 64.8
Cancer cells 1.05
MOUSE CELLS 91.9
T cells 6.78
MYC - 55.1
MYC + 29.2
CD127+ 18.1
Cancer cells 34.3
T cells 0.51
MOUSE CELLS 41.9
MYC- 62.9
MYC+ 14.0
CD127+ 78.6
CD3
CD45
myc
CD127
g
T cell count/mL
CAR-T cell count/mL
Cancer cell count/mL
CD127% on cancer cell
cell number
cell %
KO
UT
L28Z
H28Z
nd
*

Supplementary Fig. S8. Knockout LOW CAR T cells are efficacious at a low dose against high- and low-antigen-expressing T-ALL cell lines DND.41 and HPB-ALL. a, Schematic of the *in vivo* study design. Mice were inoculated with $3x10^6$ DND.41-effLuc cells intravenously, followed 4 days later by intravenous administration of $1x10^6$ wild-type LOW (solid light blue) or knockout LOW (dashed light blue) CAR T cells (left panel). Tumor burden BLI was analyzed by use of 2-way analysis of variance (right panel). Data represent results from 9 mice per group. **b,** Schematic of the *in vivo* study design. Mice were inoculated intravenously with $3x10^6$ DND.41-effLuc cells, followed 16 days later by intravenous administration of $1x10^6$ CAR T cells. Data represent results from 3 mice per group. **c,** Representative flow cytometry density plots (left panel) showing the presence of T cells ($CD45^{hi}$ $CD3^+$) and residual tumor cells ($CD45^{dim}$ $CD3^-$) detected in blood, spleen, liver, and bone marrow (BM) on day 34 after administration of CAR T cells. Corresponding summary data plots show the percentage of cancer cells, total T cells, and CAR T cells (right panel). Data are representative of 3 mice and are presented as mean ± standard error of the mean. Statistical analysis was performed using unpaired two-tailed Student's t-tests. No statistically significant differences were observed between groups. **d,** Schematic of the *in vivo* study design. Mice were inoculated with $3x10^6$ HPB-ALL-effLuc cells intravenously, followed 4 days later by intravenous administration of $3x10^6$ CAR T cells. **e,** Histogram plot showing the expression of endogenous CD127 (percentage and MFI) on HPB-ALL cancer cells. Data are representative of 3 independent experiments. **f,** Representative flow cytometry density plots showing the percentage of total T cells ($CD45^+$ $CD3^+$) and CAR T cells (MYC^+ $CD45^+$ $CD3^+$) and histogram plots showing expression of CD127 on residual tumor cells ($CD3^+$ $CD45^-$) harvested from spleen on day 30 after administration of CAR T cells. Data are representative of 3 mice. **g,** Summary plots showing the quantification of T-cell, CAR T-cell, and cancer cell counts, and the percentage of CD127-expressing cancer cells. Data are presented as mean ± standard deviation. Number of mice: KO UT (n = 4), KO LOW (n = 4), and KO HIGH (n = 4). Statistical analysis was performed using multiple unpaired two-tailed Student's *t*-tests. Exact p values (KO LOW vs KO HIGH)**:** T-cell count, $p = 0.3252$; CAR T-cell count, $p = 0.3276$; Cancer cell count, $p = 0.0423$; CD127 expression on cancer cells, $p = 0.0005$. D, day; KO, knockout; ns, not significant; wo, washout; WT, wild-type. Source data are provided as source data file.

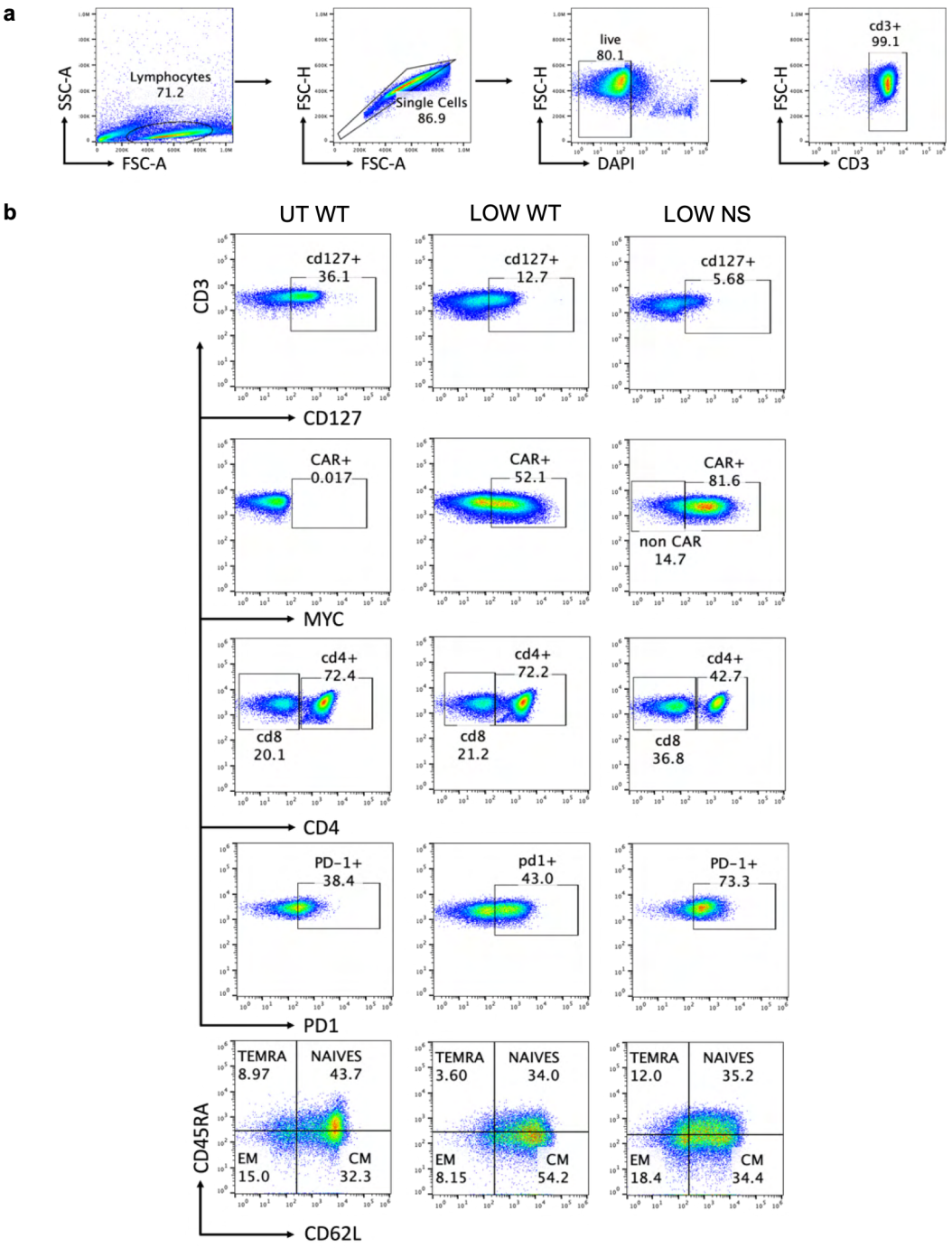

Supplementary Fig. S9. Supplementary data supporting the data presented in Fig. 6. a, Fig. 7c and 7d, Gating strategy of flow cytometry analysis performed in Fig. 6b-d and **b,** representative flow cytometry dot plots showing the percentage of CAR expression ($CD3^+$ $CD45^+$ MYC^+) and CD127, CD4, and PD-1 percentage. The memory cell phenotypes of CAR T cells were determined as naive ($CD45RA^+$ $CD62L^+$), central memory (CM; $CD45RA^-$ $CD62L^+$), effector memory (EM; $CD45RA^-$ $CD62L^-$), and terminal effector memory ($CD45RA^+$ $CD62L^-$) cell subtypes. FSC-A, forward scatter area; FSC-H, forward scatter height; NS, naturally selected; SSC-A, side scatter area; WT, wild-type.

a

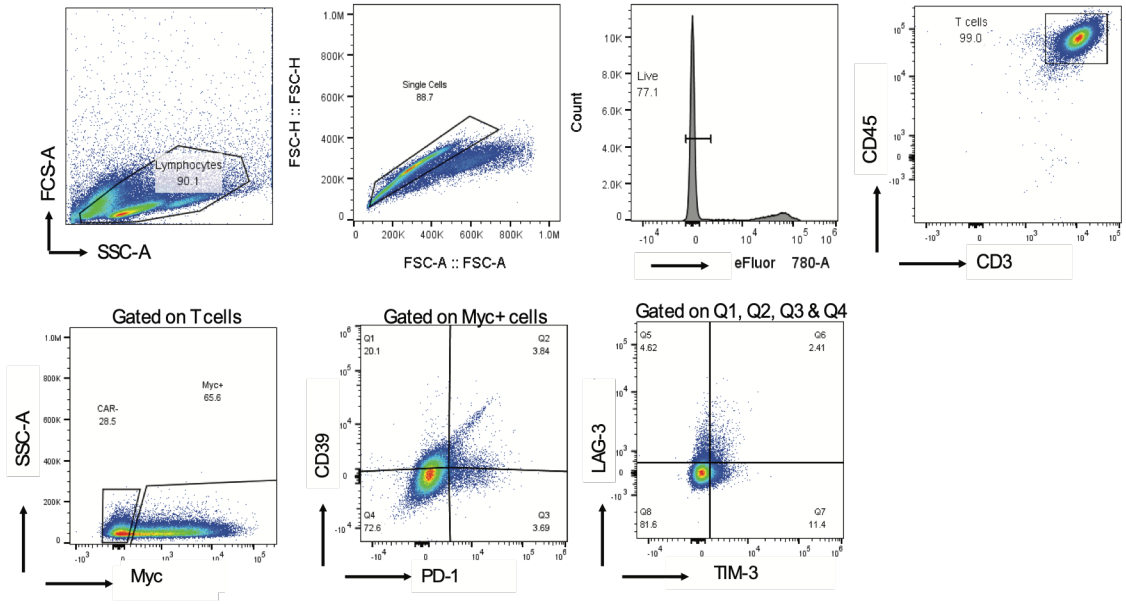

Supplementary Fig. S10. Gating strategy and cell phenotype plots of the data presented in Fig. 6g and Fig. 7. e, Gating strategy used for flow cytometric analysis of CAR T-cell phenotype and exhaustion marker expression. Representative flow cytometry plots show sequential gating on lymphocytes (FSC-A versus SSC-A), singlets (FSC-H versus FSC-A), viable cells (eFluor 780^{-}), and T cells ($CD3^{+}CD45^{+}$). CAR T cells were identified based on Myc-tag expression (Myc^{+}). Within the CAR T-cell population, expression of exhaustion-associated markers PD-1, CD39, TIM-3, and LAG-3 was assessed. Representative quadrant gates used to define PD-1 and CD39 expression, as well as TIM-3 and LAG-3 co-expression, are shown. FSC-A, forward scatter area; FSC-H, forward scatter height; SSC-A, side scatter area.

a

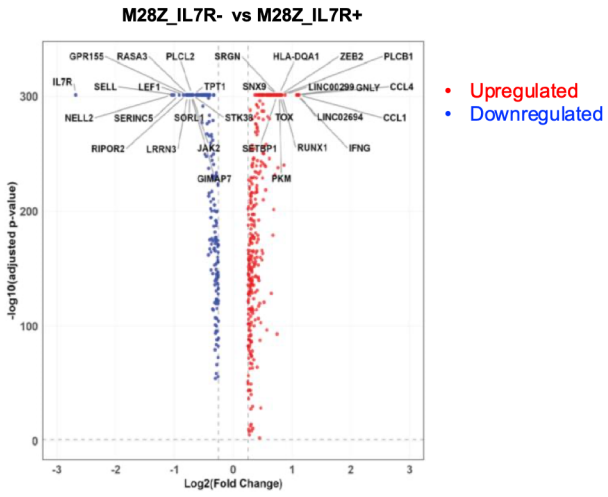
M28Z_IL7R- vs M28Z_IL7R+
GPR155
RASA3
PLCL2
SRGN
HLA-DQA1
ZEB2
PLCB1
IL7R
SELL
LEF1
TPT1
SNX9
LINC00299
GNLY
CCL4
NELL2
SERINC5
SORL1
STK38
TOX
LINC02694
CCL1
RIPOR2
LRRN3
JAK2
SETBP1
RUNX1
IFNG
GIMAP7
PKM
-log10(adjusted p-value)
Log2(Fold Change)
Upregulated
Downregulated

b

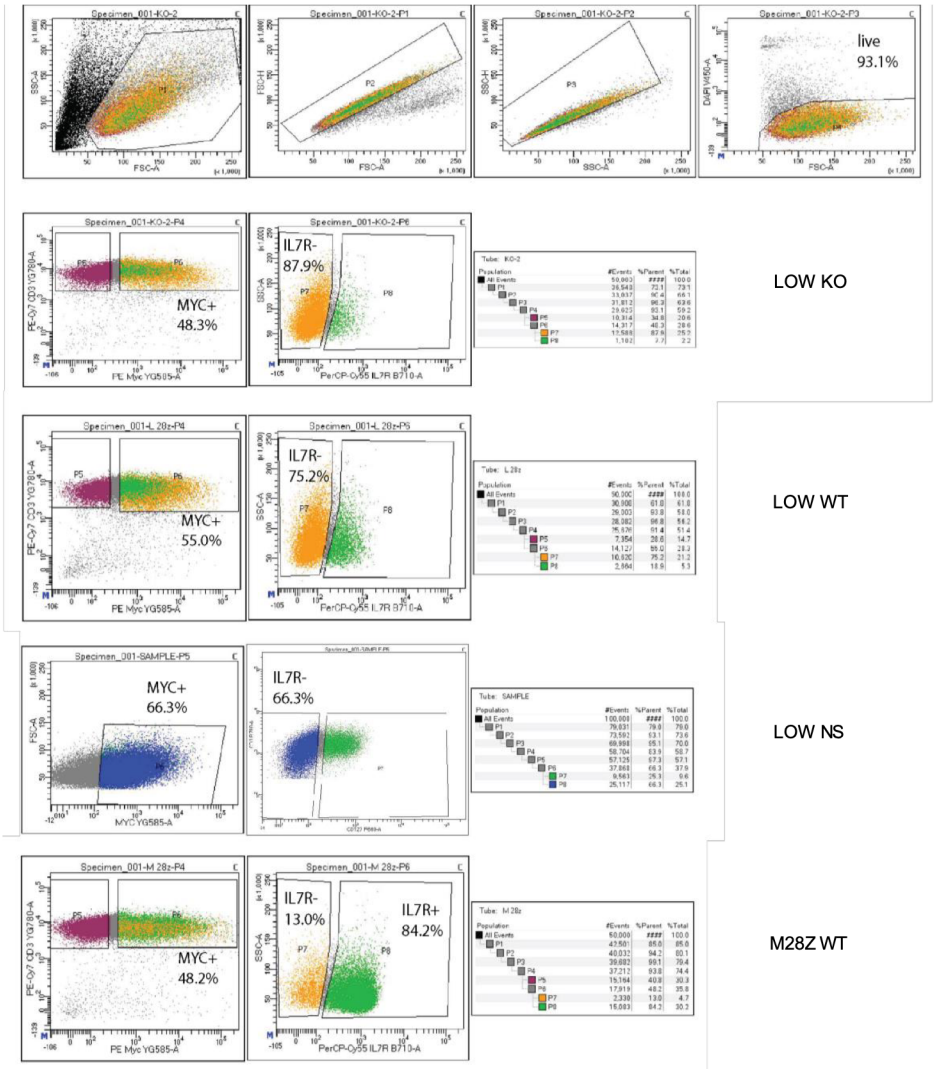
live
93.1%
MYC+
48.3%
IL7R-
87.9%
LOW KO
MYC+
55.0%
IL7R-
75.2%
LOW WT
MYC+
66.3%
IL7R-
66.3%
LOW NS
MYC+
48.2%
IL7R-
13.0%
IL7R+
84.2%
M28Z WT

Supplementary Fig. S11. Supplementary data supporting the data presented in Supplementary Fig. S12. a, Volcano plot comparing gene expression changes between M28Z MYC^+ $IL7R^-$ and M28Z MYC^+ $IL7R^+$ CAR T cells. The x-axis represents the log_2 fold change in wild-type CAR T cells, and the y-axis represents the log_2 fold change in naturally selected CAR T cells. Upregulated genes are shown in red; downregulated genes are shown in blue. The top 15 differentially expressed genes are labeled within the samples. RNA sequencing was performed on cells isolated from a single donor. **b,** Representative flow cytometric analysis illustrating the gating strategy used to sort the 5 cell populations analyzed by RNA sequencing. FSC-A, forward scatter area; FSC-H, forward scatter height; KO, knockout; NS, naturally selected; P, patient; SSC-A, side scatter area; SSC-H, side scatter height; WT, wild-type.

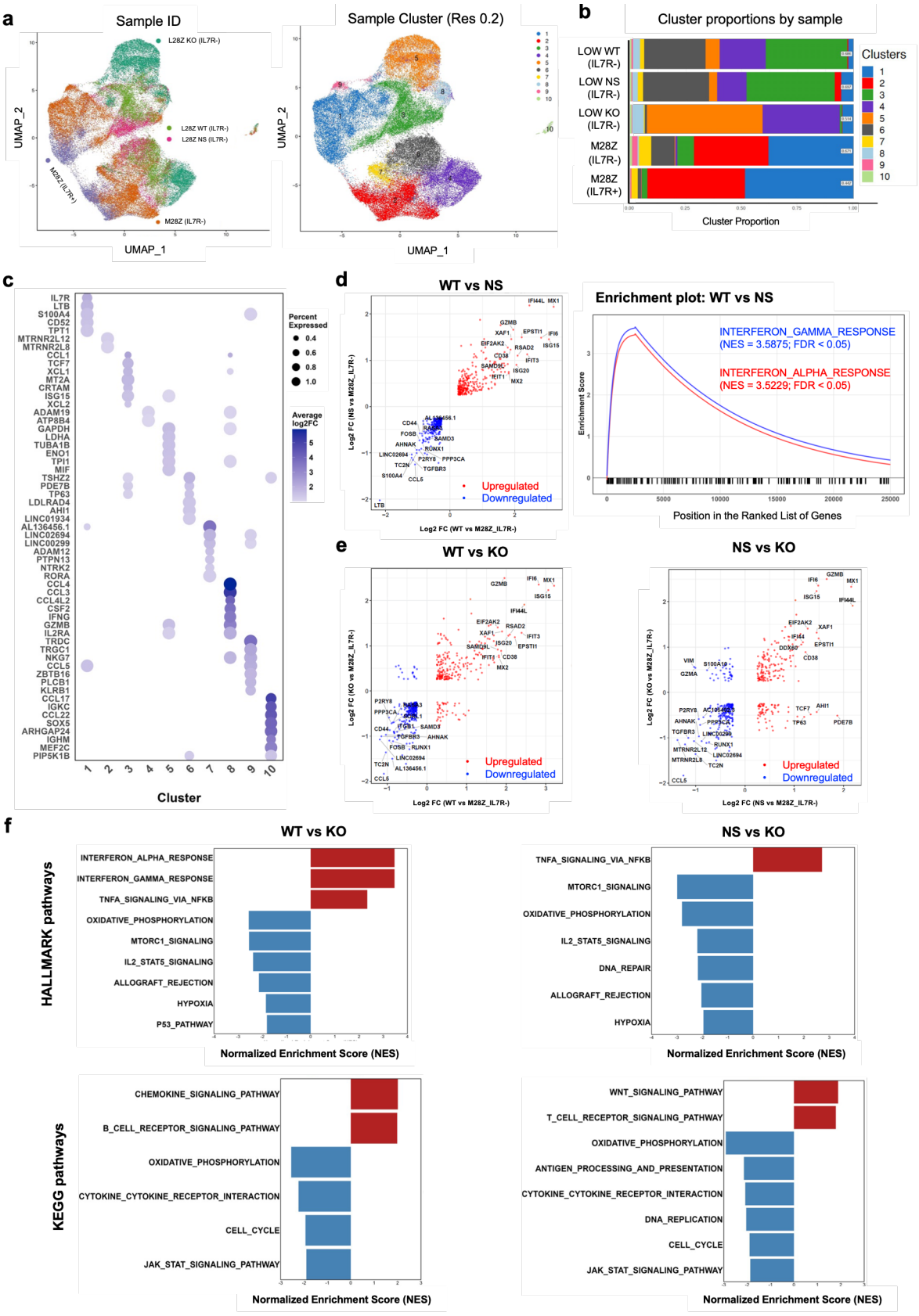
a
Sample ID
L28Z KO (IL7R-)
L28Z WT (IL7R-)
L28Z NS (IL7R-)
M28Z (IL7R+)
M28Z (IL7R-)
UMAP_1
UMAP_2
Sample Cluster (Res 0.2)
b
Cluster proportions by sample
LOW WT (IL7R-)
LOW NS (IL7R-)
LOW KO (IL7R-)
M28Z (IL7R-)
M28Z (IL7R+)
Clusters
Cluster Proportion
c
Percent Expressed
Average log2FC
Cluster
d
WT vs NS
Log2 FC (WT vs M28Z_IL7R-)
Log2 FC (NS vs M28Z_IL7R-)
Upregulated
Downregulated
Enrichment plot: WT vs NS
INTERFERON_GAMMA_RESPONSE
(NES = 3.5875; FDR < 0.05)
INTERFERON_ALPHA_RESPONSE
(NES = 3.5229; FDR < 0.05)
Enrichment Score
Position in the Ranked List of Genes
e
WT vs KO
NS vs KO
Log2 FC (KO vs M28Z_IL7R-)
Log2 FC (WT vs M28Z_IL7R-)
Log2 FC (NS vs M28Z_IL7R-)
f
WT vs KO
NS vs KO
HALLMARK pathways
INTERFERON_ALPHA_RESPONSE
INTERFERON_GAMMA_RESPONSE
TNFA_SIGNALING_VIA_NFKB
OXIDATIVE_PHOSPHORYLATION
MTORC1_SIGNALING
IL2_STAT5_SIGNALING
ALLOGRAFT_REJECTION
HYPOXIA
P53_PATHWAY
DNA_REPAIR
Normalized Enrichment Score (NES)
KEGG pathways
CHEMOKINE_SIGNALING_PATHWAY
B_CELL_RECEPTOR_SIGNALING_PATHWAY
CYTOKINE_CYTOKINE_RECEPTOR_INTERACTION
CELL_CYCLE
JAK_STAT_SIGNALING_PATHWAY
WNT_SIGNALING_PATHWAY
T_CELL_RECEPTOR_SIGNALING_PATHWAY
ANTIGEN_PROCESSING_AND_PRESENTATION
DNA_REPLICATION

Supplementary Fig. S12. Single-cell RNA-sequencing analysis of low-affinity CD127-targeted LOW CAR T cells reveals differential gene expression and pathway enrichment. Low-affinity CD127-targeted LOW CAR T cells were collected on day 5 (LOW wild-type and LOW knockout, along with control M28Z wild-type) or day 10 (LOW NS) and sorted for MYC^{+} $IL7R^{-/+}$ and subjected to single-cell RNA-sequencing analysis to profile gene expression. **a,** Uniform manifold approximation and projection (UMAP) plot of pooled CAR T cells from all 5 samples, identifying 10 clusters at a resolution of 0.2, on the basis of differentially expressed genes. **b,** Bar plots showing the proportion of each cluster within the samples. **c**, Bubble plots displaying significant genes associated with each cluster, where the bubble color represents the normalized expression level and bubble size indicates the percentage of cells expressing the gene. **d,** Volcano plot comparing gene expression changes between wild-type and naturally selected CAR T cells, normalized to M28Z (MYC^{+} $IL7R^{-}$). The x-axis represents the $\log_2$ fold change in wild-type CAR T cells, and the y-axis represents the $\log_2$ fold change in naturally selected CAR T cells. Upregulated genes are shown in red; downregulated genes are shown in blue. The top right quadrant highlights genes upregulated in both wild-type and naturally selected CAR T cells; the bottom left quadrant shows genes downregulated in both. The right panel presents gene set enrichment analysis for IFNα and IFNγ gene sets, with normalized enrichment score (NES) and false discovery rate (FDR) values indicated. **e,** Volcano plot comparing gene expression changes between wild-type and knockout CAR T cells. The top left quadrant highlights genes upregulated in knockout but not in wild-type CAR T cells; the bottom right quadrant shows genes upregulated in wild-type but not in knockout CAR T cells. A similar volcano plot compares naturally selected and knockout CAR T cells, with gene expression normalized to M28Z (MYC^{+} $IL7R^{-}$). Significantly enriched genes (fold change >1) are labeled. **f,** Gene set enrichment analysis for HALLMARK and KEGG pathway analysis between wild-type and knockout CAR T cells and between naturally selected and knockout CAR T cells. Normalized enrichment score values are indicated, with upregulated gene sets shown in red and downregulated gene sets shown in blue. FC, fold change; KO, knockout; NS, naturally selected; WT, wild-type. Source data are provided as source data file.

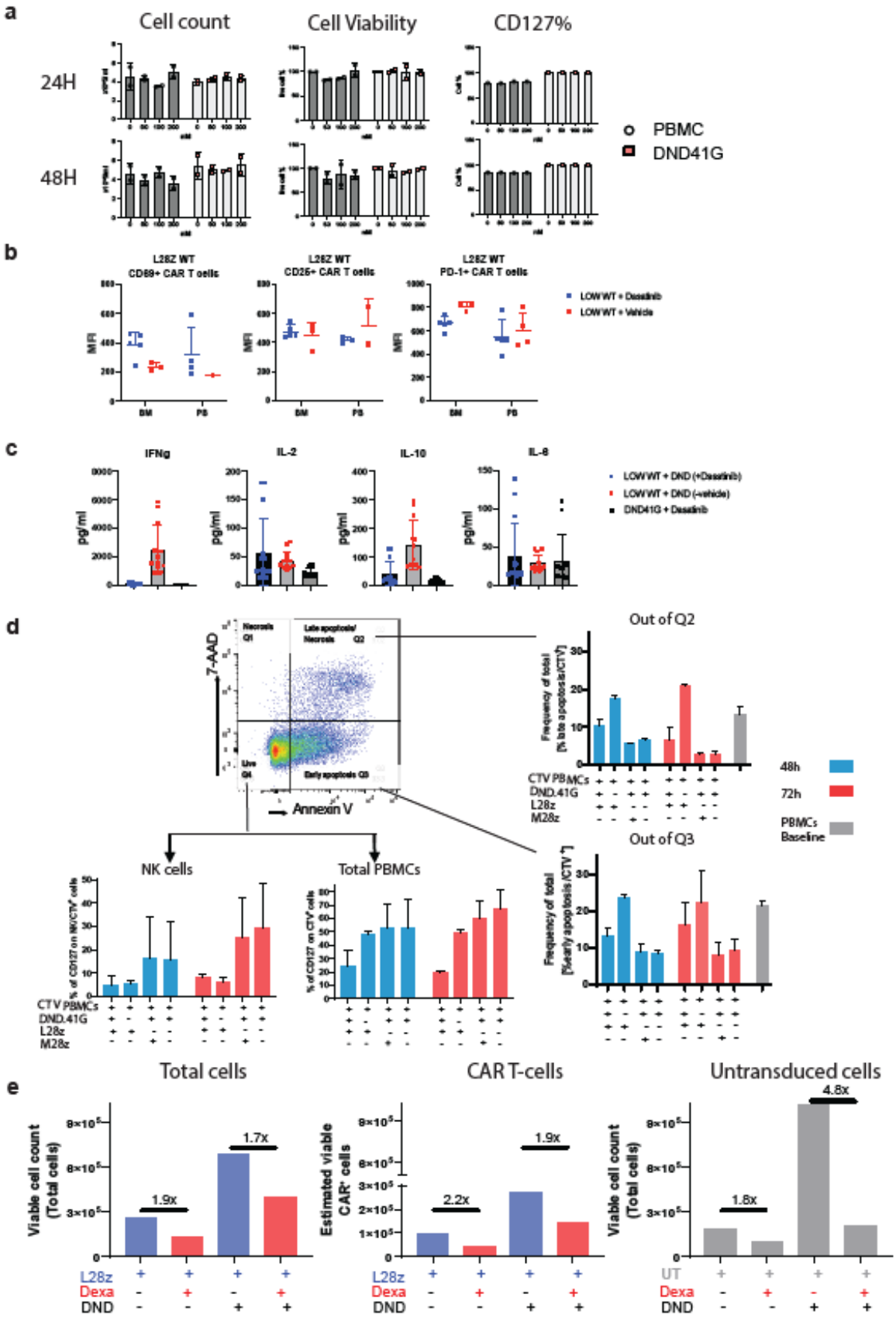
a
Cell count
Cell Viability
CD127%
24H
48H
PBMC
DND41G
b
L28Z WT
CD69+ CAR T cells
L28Z WT
CD25+ CAR T cells
L28Z WT
PD-1+ CAR T cells
MFI
BM
PB
LOWWT + Dasatinib
LOWWT + Vehicle
c
IFNg
IL-2
IL-10
IL-8
pg/ml
LOWWT + DND (+Dasatinib)
LOWWT + DND (-vehicle)
DND41G + Dasatinib
d
7-AAD
Annexin V
Necrosis
Q1
Late apoptosis/
Necrosis
Q2
Live
Q4
Early apoptosis Q3
Out of Q2
Out of Q3
Frequency of total
(% late apoptosis/CTV+)
Frequency of total
(%early apoptosis /CTV+)
CTV PBMCs
DND.41G
L28z
M28z
48h
72h
PBMCs
Baseline
NK cells
Total PBMCs
% of CD127 on NK/CTV+ cells
% of CD127 on CTV+ cells
e
Total cells
CAR T-cells
Untransduced cells
Viable cell count
(Total cells)
Estimated viable
CAR+ cells
1.9x
1.7x
2.2x
1.9x
1.8x
4.8x
L28z
Dexa
DND
UT

Supplementary Fig. S13. Supplementary data supporting the data presented in Fig. 7. a, Comparison of the *in vitro* cell count, cell viability, and percentage of cells expressing CD127 in healthy donor–derived PBMCs and target cells (DND.41G) at 24 h (top panel) and 48 h (bottom panel) after exposure to dasatinib at concentrations of 0 to 200 nM, respectively. Data are based on 2 technical replicates. **b,** MFI signal of expression of early activation markers CD69, CD25, and PD-1 on CAR T cells detected in bone marrow (BM) and peripheral blood (PB) harvested on day 9. Number of donors: BM: LOW WT + Dasatinib (n = 5) and LOW WT + Vehicle (n = 3) for all markers. PB: CD69, LOW WT + Dasatinib (n = 4) and LOW WT + Vehicle (n = 1); CD25, LOW WT + Dasatinib (n = 3) and LOW WT + Vehicle (n = 2); PD-1, LOW WT + Dasatinib (n = 5) and LOW WT + Vehicle (n = 4). Data are presented as mean ± standard error of the mean. **c,** Cytokine secretion in serum collected on day 9 after administration of CAR T cells assessed by Luminex assay, showing the concentration of proinflammatory and immunosuppressive cytokines IFN**γ**, IL2, IL10, and IL6. WT, wild-type. Number of donors: n = 15 for LOW WT + DND + Dasatinib, n = 12 for LOW WT + DND + vehicle, and n = 12 for DND41G + Dasatinib. **d,** On-target off-tumor killing of low-affinity CD127 CAR T cells in autologous co-culture assays. Representative flow-cytometry plots showing gating strategy for live (Annexin V^- 7-AAD^-), early apoptotic (Annexin V^+ 7-AAD^-), and late apoptotic/necrotic (Annexin V^+ 7-AAD^+) CTV-labeled PBMCs following co-culture with CAR T cells. Bar graphs show quantification of live and apoptotic fractions among CTV^+ PBMCs at 48 and 72 h. Data represent 2 independent donors and are presented as mean ± standard deviation. **e**, effect of dexamethasone on CAR T-cell expansion. Estimated CAR^+ cell numbers were calculated from total viable counts adjusted by CAR expression measured by flow cytometry at 72 h. In the absence of tumor targets, dexamethasone reduced CAR^+ cell numbers (~2.2-fold). In the presence of DND41 cells, a similar reduction was observed (~1.9-fold). Comparable trends were observed in untransduced (UT) T cells cultured under the same conditions. Data are representative of 2 independent donors.

Supplementary Table 1. Patient characteristics. Samples from pediatric and adult patients with T-cell acute lymphoblastic leukemia (T-ALL) were obtained at different stages of treatment. Data for patient 13 not shown here. BM, bone marrow; ETP-ALL, early T-cell precursor acute lymphoblastic leukemia; PB, peripheral blood.

Patient No.	Age	Diagnosis	Sample	Treatment Course
1	Adult	ETP-ALL	PB	Diagnostic
2	Adult	T-ALL	BM, PB	Diagnostic
3	Adult	T-ALL	PB	Diagnostic
4	Pediatric	T-ALL	BM	Mid Treatment/Relapse
5	Pediatric	T-ALL	BM	Post Treatment
6	Pediatric	ETP-ALL	BM	Remission
7	Pediatric	ETP-ALL	PB	Mid Treatment/Relapse
8	Pediatric	ETP-ALL	PB	Mid Treatment
9	Adult	ETP-ALL	PB	Mid Treatment/Relapse
10	Adult	T-ALL	BM	Mid Treatment/Relapse
11	Adult	T-ALL	PB	Mid Treatment
12	Adult	T-ALL	BM	Mid Treatment
13	—	—	—	—
14	Adult	T-ALL	PB	Mid Treatment
15	Adult	T-ALL	PB	Diagnostic
16	Adult	T-ALL	PB	Post Treatment
17	Adult	ETP-ALL	PB	Post Treatment
18	Adult	T-ALL	PB	Diagnostic
19	Adult	T-ALL	PB	Post Treatment
20	Adult	ETP-ALL	PB	Diagnostic
21	Adult	T-ALL	PB	Mid Treatment/Relapse
22	Adult	T-ALL	PB	Diagnostic

Supplementary Table 2. Human monoclonal antibodies and reagents used for flow cytometric analysis

Target	Fluorescence	Clone	Supplier	Catalog No.	Dilution
CD3	Pe-Cy7	SK3	Biolegend	344816	1:100
	APC-Cy7	OKT-3	Biolegend	317342	1:100
	BV650	OKT-3	Biolegend	317324	1:100
CD8	AF700	SK1	Biolegend	344724	1:100
	Pe-Cy7	RPA-T8	BD BioScience	557746	1:100
CD4	AF700	SK3	Biolegend	344622	1:100
	AF700	RPA-T4	BD BioScience	557922	1:100
	PE-CF 594	RPA-T4	BD BioScience	562281	1:100
CD127	APC	A019D5	Biolegend	351316	1:50
Myc tag	PE	9B11	Cell Signal.Tech	3739S	1:100
PD1 (CD279)	BV711	EH12.2H7	Biolegend	329928	1:50
	Pe-Cy7	EH12.2H7	Biolegend	329917	1:50
	APC	EH12.2H7	Biolegend	329928	1:50
CD45	FITC	2D1	Biolegend	368508	1:100
	Percp-Cy5.5	2D1	Biolegend	368504	1:100
CD45RA	Pe-dazzle 594	HI100	Biolegend	983008	1:50
	Percp-Cy5.5	HI100	Biolegend	304122	1:50
	FITC	HI100	Biolegend	304106	1:50
CD25	FITC	BC96	Biolegend	302604	1:100
CD62L	Pe-Cy7	DREG-56	Biolegend	304822	1:50
	FITC	DREG-56	Biolegend	555543	1:50
	PE-CF 594	DREG-56	BD BioScience	562301	1:50
Tim3 (CD366)	PE	F-38E2	Biolegend	345005	1:50
	BUV737	7D3	BD BioScience	748820	1:50
CD7	PE	CD7-6B7	Biolegend	343106	1:100
	FITC	CD7-6B7	Biolegend	343104	1:100
CD2	Pe-Cy7	RPA-2.10	Biolegend	2215976	1:100
CD14	PE-eFluor 610	61D3	Invitrogen	2082413	1:100
CD5	APC-eFluor 780	UCHT-2	Invitrogen	2202488	1:100
CD34	APC-Cy7	561	Biolegend	343613	1:100
CD39	BB700	TU66	BD BioScience	745904	1:50
LAG3 (CD223)	Percp-Cy5.5	11C3C65	Biolegend	369312	1:50
IFNg	APC	B27	BD BioScience	554702	1:50
CD69	Pe-Cyanine 5	H1.2F3	Biolegend	104510	1:100
CD19	BV711	HIB19	Biolegend	302245	1:100
CD107a	AF700	H4A3	BD BioScience	561340	1:50
PDL1 (CD274)	FITC	MIH2	Biolegend	393606	1:50
IL-2	APC	MQ1-17H12	Thermo Fisher	14-7029-81	1:50
TNFa	FITC	Mab11	Thermo Fisher	11-7349-82	1:50
DAPI			Thermo Fisher	WI3371931	1 μg mL^{-1}
7AAD			Biolegend	420404	5 uL per 10^6 cells

Human FcR blocker	Miltenyi Biotec	130-059-901	5 uL per 10^7 cells
Mouse FcR blocker	Miltenyi Biotec	130-092-575	5 uL per 10^7 cells